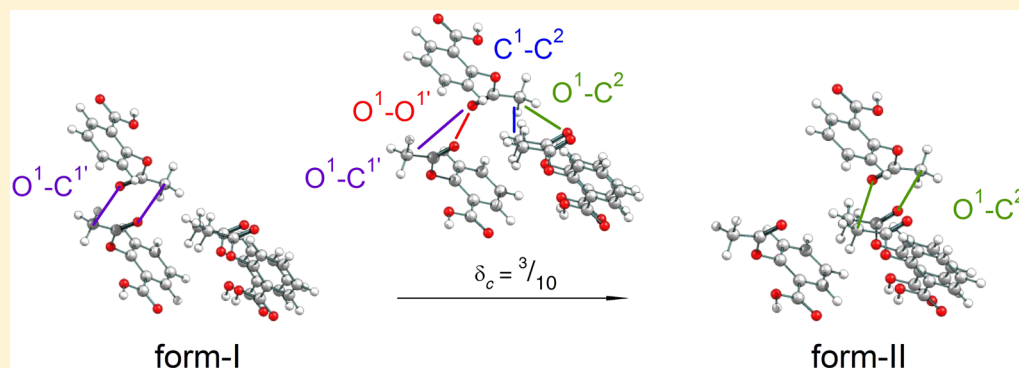


Evaluation of Shear-Slip Transitions in Crystalline Aspirin by Density-Functional Theory

Luc M. LeBlanc,^{*,†} Alberto Otero-de-la-Roza,^{*,‡} and Erin R. Johnson^{*,†}[†]Department of Chemistry, Dalhousie University, 6274 Coburg Road, P.O. Box 15000 Halifax, Nova Scotia, Canada B3H 4R2[‡]Department of Chemistry, University of British Columbia, Okanagan, 3247 University Way, Kelowna, British Columbia, Canada V1V 1V7

S Supporting Information



ABSTRACT: Crystalline aspirin has been shown to form two distinct polytypes, or polymorphs, that differ only in one unit-cell dimension. The second polytype is metastable and has been proposed to convert to the original form through a one-dimensional shear-slip mechanism. The feasibility of the $\{100\}\langle 001\rangle$ shear-slip system, relating the two known aspirin forms, is examined computationally by the use of periodic-boundary density-functional theory (B86bPBE-XDM). A low barrier of ca. 10 kJ/mol per molecule is computed, which is estimated to be consistent with the observed interconversion rate, accounting for uncertainties in the treatment of thermal effects. The barrier is shown to increase under applied pressure, explaining previous experimental observations that compression of aspirin-II did not result in reversion to aspirin-I under the time scales considered. Finally, the advisability of using aspirin, or other compounds that form similar polytypes, as tests of computational methods for studies of polymorphism is discussed. Because of their high geometric similarity, both polytypes are predicted to be effectively degenerate regardless of the treatment of intermolecular dispersion.

■ INTRODUCTION

Aspirin (*o*-acetylsalicylic acid)¹ has received considerable attention over the past decade, largely due to the prediction of a second nearly degenerate polymorphic crystalline form² and the subsequent work leading to its isolation in “pure” form.^{3–7} This second form, further referred to as aspirin-II or form-II, is nearly energetically degenerate to the first solved crystal structure¹ (aspirin-I or form-I), with the lattice-energy difference between the two forms being less than half a kJ/mol.^{8,9}

The structural differences between the two crystal forms are subtle. In both forms, aspirin molecules are arranged in centrosymmetric dimers, interacting via strong carboxyl O–H...O hydrogen bonds, which are then arranged in bilayers propagating along the *bc*-plane. The bilayers are periodically stacked along the *a*-axis. Along the *c*-axis, neighboring dimers have alternating orientations and are inclined with respect to the *ac*-plane.^{10,11}

One of the key differences between the two forms, shown in Figure 1a, lies in whether the pseudo-hydrogen-bonding C–H...O motif between the interacting acetyl and carboxyl groups of two neighboring bilayers along the *b*-axis is dimeric (form-I, inversion

centers) or catemeric (form-II, 2₁ screw axes).^{3,12} Indeed, these similar interactions have been proposed as the reason for the near-degeneracy of the two forms of aspirin. Form-I possesses the more-favorable intramolecular conformation, while intermolecular C–H...O bonding cooperativity favors form-II.⁸ The other difference lies in the observation that two neighboring layers of aspirin dimers along the $\{100\}$ plane are related by translation of one layer relative to the other by $(1/2)\cdot c$ along the crystallographic *c*-axis, as shown in Figure 1b.^{4–7,11}

The relationship between the two forms makes choosing the proper unit cell crucial during refinement of X-ray diffraction data, as was illustrated by an unsatisfactory analysis of the data and the premature claim that aspirin-II could be prepared as a stable crystalline solid.^{3,4} This was closely followed by a proposal of an intergrowth structure for aspirin, in which domains of form-I and form-II are present within the same crystal in variable ratios.⁵

Received: July 12, 2016

Revised: September 22, 2016

Published: October 17, 2016



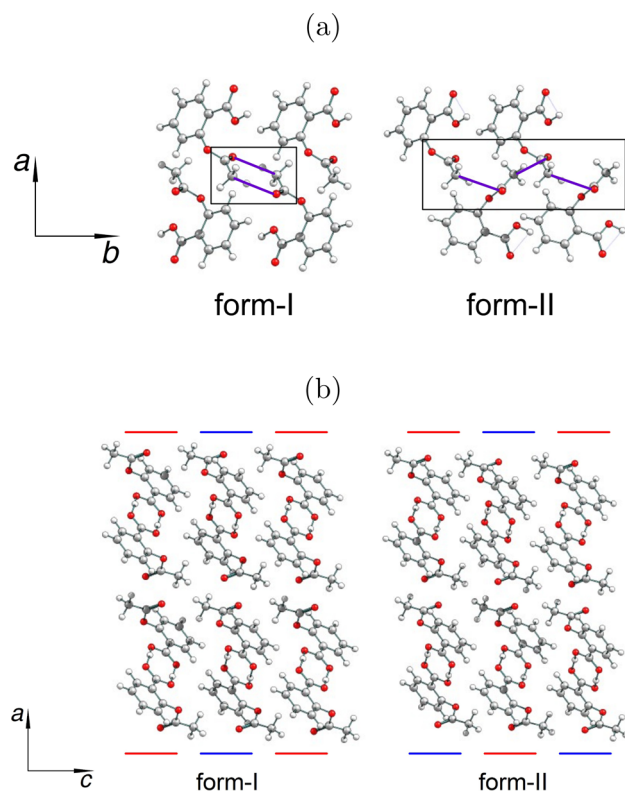


Figure 1. Key structural differences between the two forms of aspirin. (a) Dimer/catemer motifs viewed along the *b*-axis. (b) 2D bilayers of aspirin dimers viewed along the *c*-axis. The red and blue lines highlight the different molecular orientations with respect to the *ac*-plane.

Crystal composition and disorder in these intergrowth structures were later found to be detectable by the extent of diffuse scattering and/or streaks in the diffraction patterns.^{5,10,13}

The mechanical stability (or instability) of the two forms has also been debated in multiple experimental^{3,6,7,11,14} and computational^{2,14,15} studies. The initial prediction of the form-II structure was accompanied by the calculation of a low shear coefficient (using an analytic second-derivatives method for rigid molecules and anisotropic atom–atom potentials as implemented in the DMAREL crystal structure modeling program).¹⁶ This supported its mechanical instability and potential conversion to form-I, if the latter turned out to be thermodynamically favored.² However, other studies of the elastic and thermal properties,¹⁴ including density-functional computation of the bulk and shear modulus values,¹⁵ have since showed no evidence of shear instability.

In 2011, a method for the preparation of “pure” aspirin-II (to the detection limit of the X-ray diffraction method used) was reported by crystallizing aspirin in the presence of aspirin anhydride.⁶ Studies of these single crystals at pressures of up to 2.2 GPa indicated no phase transition from form-II to form-I, thus providing another piece of evidence for the mechanical stability of the new form.⁶ A recent experimental study on the behavior of both forms of aspirin under higher pressures was conducted and coupled with micro-Raman spectroscopy.¹¹ Echoing previously published results,⁶ no phase transition was observed¹¹ even upon application of pressures of up to 10 GPa to aspirin-II crystals, which is consistent with the established behavior of the CPA-A and CPA-C polymorphs of chlorpropamide under similar conditions.¹⁷ However, the use of a nano-indentation technique on these “pure” form-II crystals led to the

detection of form-I domains in some of the form-II crystals produced.⁷ It was further noted that these crystals would convert to aspirin-I over a period of several months through the observation that characteristic peaks for form-II would disappear over time in X-ray diffraction spectra of bulk powders stored under ambient conditions. When subjecting these same crystals to mechanical grinding (i.e., under the influence of shear stress), quick transformation from form-II to form-I took place.⁷ This implies that slip along the $\{100\}\langle 001 \rangle$ system in aspirin is the most likely phase-transition mechanism between the two forms. Additionally, calculations of attachment energies between adjacent dimeric layers along the *a*-axis (using the Dreiding force field model) also revealed the $\{100\}$ planes to be the most weakly bound and thus more susceptible to slip,⁷ in agreement with previous models for calculating attachment energies in organic solids.¹⁸

To summarize, the near-degeneracy of both forms of aspirin and the evaluation of their thermodynamic stabilities^{8,9,15} supports the formation of intergrowth structures.^{5,19} It does not, however, give sufficient foundation to explain the metastability of form-II and its eventual conversion to form-I under ambient conditions in the presence or absence of shear stress.⁷ Investigation of the potential ease with which interconversion between polymorphic forms through slip systems along one dimension (i.e., polytypes) can occur is necessary to better understand this class of compounds.

In this work, we aim to resolve contrasting experimental and computational results of whether or not form-II is mechanically stable under compression or shear stress. The viability of the $\{100\}\langle 001 \rangle$ slip mechanism is considered using periodic-boundary density-functional theory (DFT). The barriers for interconversion between the two forms, at equilibrium conditions and under pressure, are calculated and related to the observed conversion time.⁷ The limited applicability of near-degenerate, layered (i.e., polytypical) systems, such as aspirin, as benchmarks for polymorphism is also discussed.

METHODS

The crystal structures of aspirin-I and aspirin-II were retrieved from the Cambridge Structural Database (CSD).^{20,21} These were fully optimized using Quantum ESPRESSO²² version 5.1 with the projector augmented-wave (PAW) method²³ and the plane-waves/pseudopotentials approach. The cutoff energy and density were 60 and 600 Ry, respectively. A $2 \times 2 \times 2$ k-point grid was used in all cases, for both the single cells and doubled supercells (see below). The use of a denser $4 \times 4 \times 4$ k-point grid had no significant effect on the relative energies of the two forms of aspirin. Specifically, for the single cells, we found an energy difference of $\Delta E_{\text{I} \rightarrow \text{II}} = -0.29$ kJ/mol per molecule with a $2 \times 2 \times 2$ k-point grid vs -0.31 kJ/mol per molecule with a $4 \times 4 \times 4$ k-point grid.

Our calculations employed the B86bPBE functional^{24,25} with the exchange-hole dipole moment (XDM) dispersion correction,^{26–28} in which the dispersion energy is evaluated as a sum over all atomic pairs and includes C_6 , C_8 , and C_{10} terms. The values of the two parameters in the XDM damping function were set to $a_1 = 0.6512$ and $a_2 = 1.4633$ Å. To account for thermal effects in both forms of aspirin, the phonon frequencies at Γ and the corresponding phonon density of states for the relaxed structures were calculated using the phonopy program.²⁹ The vibrational Helmholtz free energies were evaluated in the harmonic approximation. Additional phonon calculations were performed on the equilibrium geometries of aspirin-I and aspirin-II to assess the convergence of the relative free energies of the two forms at 298 K with respect to finer sampling of the phonon density of states. The elastic constants, C_{ij} , and the associated Voigt-averaged shear and bulk moduli³⁰ were determined from a stress-strain methodology outlined in ref 31.

The unit cell ($Z = 4$) of aspirin-I was doubled along the $\langle 100 \rangle$ direction in order to investigate the $\{100\}\langle 001 \rangle$ slip mechanism. In this supercell, one layer of dimers was translated relative to the other in increments, δ_c , of $(1/20)c$ (c being the lattice parameter of the unit cell) along the $\langle 001 \rangle$ direction up to $(1/2)c$, i.e., resulting in a supercell of form-II. Each intermediate structure along the reaction coordinate was then optimized, allowing for relaxation of the cell. The incremented scan coordinate (the crystallographic $\langle 001 \rangle$ direction or the equivalent Cartesian z -coordinate) was frozen so as to avoid reversion to either form-I or form-II upon optimization. Because of this, the described procedure was performed starting from an aspirin-II supercell as well, in order to ensure that there was no bias due to constraints imposed by the choice of initial geometry during optimization.

RESULTS AND DISCUSSION

Relative Energetics. The experimental sublimation enthalpy is only available for aspirin-I,^{9,32} so there is no reference data for the lattice-energy difference between the two forms. The lattice energy of aspirin-I obtained with the XDM-corrected periodic-boundary DFT approach, shown in Table 1, is in fairly good

Table 1. Lattice Energies, E_{latt} in kJ/mol per Molecule, of Form-I Aspirin From Various Theoretical Methods. The Experimental Value at 0 K is Also Shown

method	E_{latt}	ref
RI-MP2/aDZ ^a	−113.7	8
RI-MP2/aTZ ^a	−132.1	8
SCS(MI) RI-MP2/aDZ ^a	−132.5	8
SCS(MI) RI-MP2/aTZ ^a	−135.6	8
MC MP2C	−116.1	9
B86bPBE-XDM	−124.2	herein
experiment	−115.0 ^b	33

^aThe RI-MP2 calculations used the many-body expansion. aDZ and aTZ indicate the aug-cc-pVDZ and aug-cc-pVTZ basis sets, respectively.

^bThis value was obtained based on the heat of sublimation of form-I of -109.7 ± 0.5 kJ/mol at 298 K.³²

agreement with the experimental result³³ (back-corrected for thermal effects) and the best reference RI-MP2 results,⁸ further supporting the good performance of DFT-XDM for molecular crystals seen in previous works.^{28,34} Additionally, the computed structural parameters (shown in the Supporting Information) are well within typical deviations from experimental data²⁰ given that thermal and vibrational contributions have been neglected.^{8,15,35}

As shown in Table 2, aspirin-I is predicted to be 0.3 kJ/mol per molecule less stable than aspirin-II with B86bPBE-XDM. Including zero-point vibrational energies decreases this difference slightly by 0.1 kJ/mol. These results compare well with previous predictions using RI-MP2,⁸ MP2C,⁹ and PBE with both the TS and many-body dispersion corrections.¹⁵ Like PBE-TS, B86bPBE-XDM predicts form-II to be marginally more stable, while the RI-MP2 calculations slightly favor form-I. However, it is not within the scope of this paper to establish the relative stability of these nearly degenerate forms to a sub-kJ/mol accuracy. Small deviations of the computational results from the nominal ordering of the two forms ($\Delta E_{\text{I} \rightarrow \text{II}} > 0$, i.e., form-I energetically favored) are certainly within the expected errors of the methods used.

Additionally, the thermodynamic preference for form-I has recently been attributed to thermal effects from the lattice vibrations, due to a change in the C–H...O pseudo-hydrogen-bonding motifs between dimeric layers along the $\{100\}$ plane.¹⁵ Accounting for thermal effects with B86bPBE-XDM and phonons calculated at the Γ -point resulted in a predicted free-energy

Table 2. Relative Energies, in kJ/mol per Molecule, of the Two Forms of Aspirin Using Selected Levels of Theory^a

method	ΔE	ΔG (0 K)	ΔG (298 K)	ref
QM/MM	−0.2			2
COMPASS MM	−1.2			14
B3LYP-D/6-31G(d,p)	−2.5			36
B3LYP-D/6-311G(d,p)	−1.9			36
B3LYP-D*/6-31G(d)	−2.5			8
B3LYP-D*/TZP	−1.4	−0.4		8
RI-MP2/aDZ ^b	0.2	−0.2		8
RI-MP2/aTZ ^b	0.1	−0.3		8
SCS(MI) RI-MP2/aDZ ^b	0.1	−0.3		8
SCS(MI) RI-MP2/aTZ ^b	0.0	−0.4		8
MC MP2C	−0.1			9
PBE-TS	−0.2	−0.4	−0.7	15
PBE-MBD	0.0	0.4	2.6	15
B86bPBE	0.2			herein
B86bPBE-XDM	−0.3	−0.2	0.3	herein

^a ΔE corresponds to the difference in electronic energies between forms II and I, i.e., $\Delta E_{(\text{I} \rightarrow \text{II})} = E_{\text{II}} - E_{\text{I}}$, whereas $\Delta G(0 \text{ K})$ and $\Delta G(298 \text{ K})$ correspond to the sum of the electronic energy, E_{el} , and the zero-point vibrational energy at 0 K, and to the sum of electronic energy with an additional thermal free-energy correction at 298 K, respectively. ^bThe RI-MP2 calculations used the many-body expansion. aDZ and aTZ indicate the aug-cc-pVDZ and aug-cc-pVTZ basis sets, respectively.

difference of 0.3 kJ/mol per molecule at 298 K, with aspirin-I now more stable than aspirin-II, following the experimental preference. Results given in the Supporting Information show that the computed thermal correction is well converged with respect to phonon sampling in the a - and c -directions. However, convergence with respect to sampling in the b -direction is much slower, and the value of the thermal correction is not converged even with a $1 \times 4 \times 1$ q -point grid. We also note that the b -direction is the one in which the unit cell is narrowest and that it is also the direction in which the C–H...O pseudo-hydrogen bonds are oriented. In light of these results, there remains a fairly large uncertainty of as much as ± 1 kJ/mol per molecule associated with the calculation of the thermal correction.

Given the high similarity of the packing arrangements and intermolecular interactions in the two forms, it is no surprise that most computational methods correctly predict them to be nearly degenerate. Indeed, in many of the cases shown in Table 2, this is likely fortuitous rather than a result of an accurate treatment of all intermolecular interactions in the lattice. In particular, the result from the B86bPBE base functional alone is already in good agreement with RI-MP2, despite the necessity of including the dispersion correction to obtain a reasonable lattice energy (the base-functional contribution to the lattice energy is only -26.1 kJ/mol for aspirin-I). High geometrical similarity will necessarily result in near energetic degeneracy, similar to what is seen for ABCABC versus ABAB stacking in graphite.^{37,38} Such polytypes will be predicted to be nearly degenerate with virtually all theoretical treatments, regardless of their treatment of intermolecular interactions, and are therefore not recommended benchmarks for computational approaches to polymorph ranking.

Finally, the elastic coefficients, along with the Voigt-averaged bulk and shear moduli, K_V and G_V , respectively, have been computed for both aspirin-I and aspirin-II and are given in the Supporting Information. The values found for the moduli of both forms are effectively the same as those previously calculated at the PBE-TS level of theory.¹⁵ These results support the

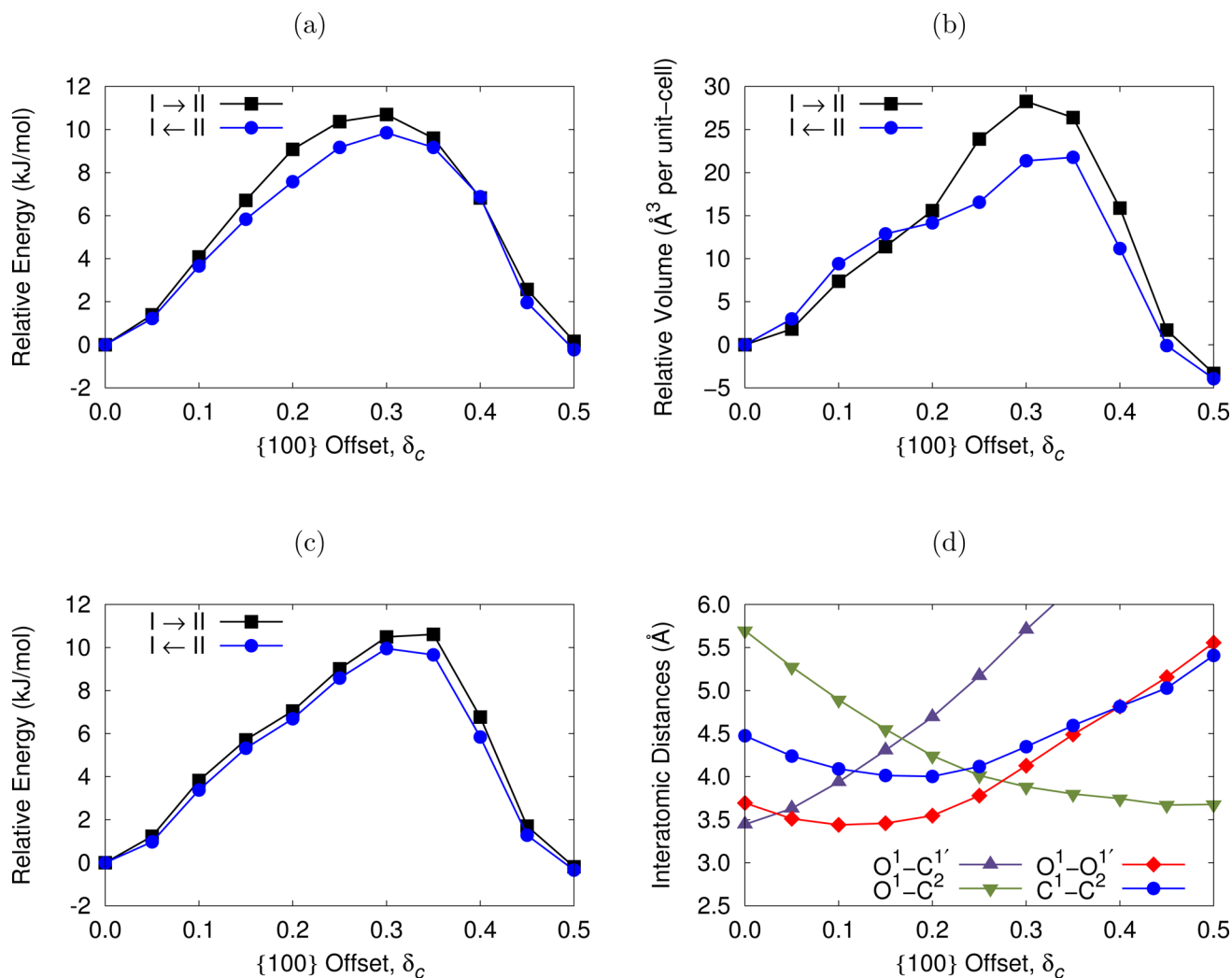


Figure 2. {100}<001> Slip mechanism in aspirin. δ_c is the slip increment along the <001> direction and is the fraction of the lattice parameter c by which both dimer layers {100} are offset. (a) PES scan for the interconversion between the aspirin-I ($\delta_c = 0$) and aspirin-II ($\delta_c = (1/2)$) crystal structures. XDM-corrected energies are given relative to aspirin-I. (b) Variation of the unit-cell volume, relative to aspirin-I, during the phase transition. (c) Minimum-energy path located for the slip mechanism using the CI-NEB method. (d) Distances between key interacting functional groups during the phase transition from aspirin-II to aspirin-I. Atom labels are shown in Figure 3.

mechanical stability of both forms, as stated in previous studies,^{14,15} and indicate that both forms are global or local minima on a corresponding potential energy surface (PES). However, while apparently stable under application of high pressures,^{6,11} aspirin-II is reported to be unstable with respect to shear stress and converts to aspirin-I after several months under ambient conditions.⁷ This implies a relatively low barrier for interconversion via a shear-slip mechanism.

Slip Mechanism. The results of the PES scan for the {100}<001> slip mechanism are presented in Figure 2a. The barriers going from form-I to form-II, and vice versa, are predicted to be 10.7 and 10.0 kJ/mol per molecule, respectively. The difference between the two barriers is due to the slightly different geometries arising from the constraining procedure employed to calculate the PES energies.

The transition state along the PES scan is located at approximately $\delta_c = (3/10)$, slightly skewed toward aspirin-II. This can be explained by the changing intermolecular interactions while sliding one layer along the <001> direction, as shown in Figures 2d and 3. First, consider aspirin-I as the starting point. In this form, the acetyl groups of aspirin interact via stabilizing

dimeric C–H \cdots O interactions. As the top layer of aspirin-I slides along the <001> direction, these interactions are weakened (depicted by the $\text{O}^1\text{--C}^{1'}$ distance in Figure 2d). This destabilization is eventually offset when the acetyl groups are brought closer to those of the neighboring molecules ($\text{O}^1\text{--C}^2$ in Figure 2d), forming the catemeric C–H \cdots O interactions seen in the aspirin-II crystal structure. The magnitude of the barrier is reasonable in light of the fact that two C–H \cdots O pseudo-hydrogen bonds are broken en route to the transition state.³⁹ For comparison, the binding energy of the formaldehyde dimer, which is bound by two analogous C–H \cdots O interactions (albeit with sp^2 rather than sp^3 carbons) is 14.3 kJ/mol.⁴⁰ Thus, the predicted barrier of ca. 10 kJ/mol per molecule is well within the realm of the expected interaction strength.

In order to further validate the results obtained with the constrained PES scan, the Nudged Elastic Band method with the Climbing-Image option enabled^{41,42} (CI-NEB) as implemented in Quantum ESPRESSO²² version 5.1 was used. An advantage to the CI-NEB method is that the points are optimized along the minimum-energy path (without reversion to the local minima), while the PES scan constrains optimization along the c -axis.

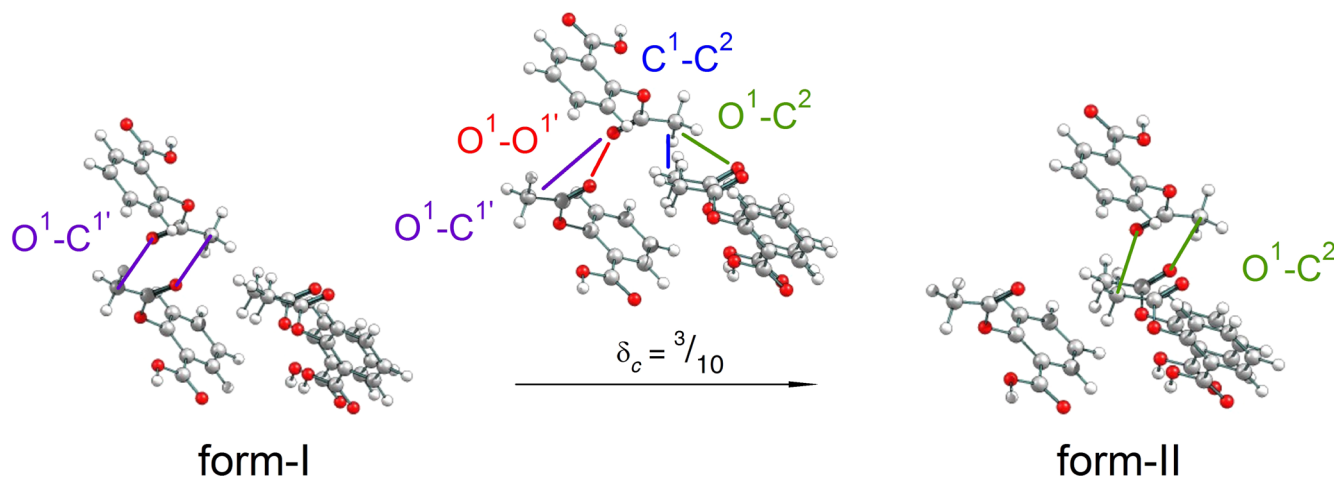


Figure 3. Variation in intermolecular interactions between the acetyl groups of aspirin during the phase transition of aspirin-I to aspirin-II via the $\{100\}\langle 001 \rangle$ slip mechanism.

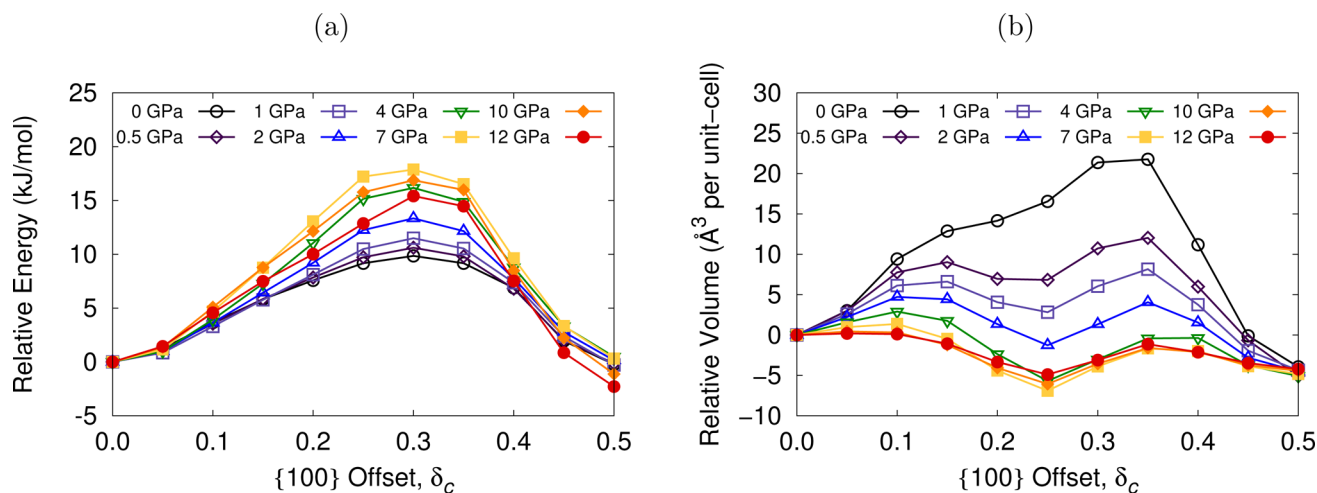


Figure 4. $\{100\}\langle 001 \rangle$ Slip mechanism in aspirin under varying pressures. (a) PES scan for the I \leftarrow II phase transition between the aspirin-I ($\delta_c = 0$) and aspirin-II ($\delta_c = (1/2)$) crystal structures for various applied pressures. Energies are given relative to aspirin-I. (b) Variation of the unit-cell volume, relative to aspirin-I, during the phase transition.

However, the NEB method implemented in Quantum ESPRESSO does not allow for variable-cell relaxation (note that a method allowing for variable-cell relaxation with the use of the NEB method has recently been implemented elsewhere.⁴³). The CI-NEB results shown in Figure 2c clearly reflect the same features of the reaction energy profile and essentially predict the same barrier, as with the constrained PES scan. The resulting barriers are 10.6 kJ/mol (I \rightarrow II) and 10.3 kJ/mol per molecule (I \leftarrow II) using 11 points along the minimum-energy path. The difference between the two barriers is due to the fixed unit-cell geometries.

Lastly, we consider whether the predicted barrier height for the $\{100\}\langle 001 \rangle$ slip mechanism is consistent with the experimental observation that aspirin-II crystals, roughly 0.1 mm in size, transform to aspirin-I over a period of several months under ambient conditions.^{6,7} Using a kinetics model for an upper bound to the conversion time for an ideal crystal via plastic deformation,⁴⁴ it can be shown that the time required for a complete conversion of an ideal crystal, with dimension \tilde{c} along the crystallographic c -axis, is given by

$$t = \left(\frac{\tilde{c}}{c} \right)^2 \frac{h}{\kappa k_B T} \left| 1 - \frac{\Delta G}{RT} \right|^{-1} e^{\Delta G/RT}$$

In this equation, ΔG is the free energy of activation for conversion of form-II supercells to form-I supercells. h , k_B , R , and T are Planck's constant, Boltzmann's constant, the gas constant, and the temperature, respectively. κ is the transmission coefficient, assumed to equal unity.

The calculated barrier for the slip mechanism in aspirin is 80 kJ/mol for the supercell composed of 8 molecules. However, the calculated barrier is the electronic-energy barrier. Estimation of the free-energy correction at the approximate transition state ($\delta_c = (3/10)$), by calculation of the phonon frequencies at Γ , reduces the barrier to 76 kJ/mol. For a crystal measuring 0.1 mm along the c -axis, this would translate to a period on the order of 27 years to undergo complete conversion. The crystal size of 0.1 mm was taken from nanoindentation experiments,⁷ but conversion is observed for a bulk powder. Considering crystal grains a quarter or a fifth of the 0.1 mm size would reduce the estimated time scale to a more realistic period of ~ 1 –2 years. Additionally, we note that there is significant uncertainty in the predicted thermal correction (potentially as large as ± 8 kJ/mol for the supercell), due to the slow convergence of the phonon density of states with respect to sampling along the b -axis as discussed above. Given the exponential dependence on the

free-energy barrier, the experimental conversion time falls well within the expected uncertainty of our calculation.

Applied Pressure. Finally, we comment on the high-pressure studies performed on the aspirin-I and aspirin-II crystals.^{6,11} These studies established that no phase transition from aspirin-II to aspirin-I occurs under high pressures (hydrostatic conditions, up to 10 GPa). These works were partly motivated by the assumption that high pressures would promote conversion of aspirin-II to aspirin-I given that the former has a slightly larger unit-cell volume at room temperature.^{7,45} As our results have shown (Figure 2b), interconversion between the two forms is accompanied by an expansion of the unit-cell volume by ca. 25 Å³ at the highest-energy point on the reaction path, which does not support this assumption. However, these results were obtained under normal pressure conditions. Conducting the same PES scan under various applied pressures (ranging from 0.5 to 12 GPa) yields the results depicted in Figure 4.

The shear-slip (electronic) energy barrier increases from ca. 10 kJ/mol per molecule, with no applied pressure, up to a maximum value of ca. 18 kJ/mol per molecule at 7 GPa (Figure 4a). This is expected on the basis that the key interacting groups at the slip interface are brought closer together due to compression and is typical of sliding processes under applied load.^{46,47}

Figure 4b shows that a local minimum in the relative unit-cell volume begins to develop near $\delta_c = (1/4)$, as the applied pressure increases. This corresponds to the region where each aspirin dimer of one layer along the *a*-axis falls exactly midway between two aspirin dimers of the adjacent layers, allowing for further compression along the $\langle 100 \rangle$ direction. Additionally, as the applied pressure surpasses 7 GPa, the energy barriers begin to decrease, which is likely due to this “interlocking” of layers. Further increases in pressure will cause greater destabilization of the C–H...O dimer and catemer interactions at $\delta_c = 0$ and $\delta_c = (1/2)$ than the interlocked contacts in the region of the transition state.

Despite the complex dependence of the shear-slip barrier on applied pressure, none of the barriers computed for pressures of up to 12 GPa fall below the barrier predicted under ambient conditions. This indicates that application of hydrostatic pressures will delay, rather than promote, the conversion of aspirin-II to aspirin-I crystals. Thus, it is no surprise that the previous high-pressure experiments^{6,11} did not reveal any indication of a phase transition between the two forms. To verify the validity of this claim would require keeping crystals of form-II aspirin under high pressures for periods longer than what was reported for the eventual conversion of the crystals under ambient conditions.^{6,7}

CONCLUSIONS

In this work, dispersion-corrected density-functional calculations were performed to investigate the relative stabilities of two polytypes of aspirin and the shear-slip mechanism for their interconversion under equilibrium conditions and under pressure. The barrier calculated with B86bPBE-XDM for the conversion between aspirin-I and aspirin-II is approximately 10 kJ/mol per molecule. Given the uncertainty in the computation of the thermal correction and the limitations of the kinetics model, this value is consistent with the observed conversion rate between the two forms of several months to a year, which is accelerated when subject to shear stress.⁷ Additionally, the computed barrier generally increases under compression, and the lowest barrier is found at zero pressure. This result explains the observed lack of conversion between aspirin-II and aspirin-I

under hydrostatic pressures up to 10 GPa within the limited time scales of the experiments.^{6,11}

We propose that nearly degenerate structures that are related by polytypism, such as the two forms of aspirin, are not good tests of the accuracy of computational methods for polymorph ranking. Given the very subtle structural differences, and thus small energy differences, between the structures being compared, almost all density functionals, even without dispersion corrections, predict a small energy difference between the two forms. Whether or not the nominal ordering is obtained is likely to be accidental.

ASSOCIATED CONTENT

Supporting Information

The Supporting Information is available free of charge on the ACS Publications website at DOI: 10.1021/acs.cgd.6b01038.

Comparison of computed and experimental structural parameters; elastic constants, Voigt-averaged bulk and shear moduli for aspirin-I and aspirin-II; convergence of the relative free-energy difference between aspirin-I and aspirin-II with respect to phonon sampling; data tables for 2D PES scans and CI-NEB calculations (PDF)

AUTHOR INFORMATION

Corresponding Authors

*(L.M.L.) E-mail: luc.leblanc@dal.ca.

*(A.O.R.) E-mail: aoterodelaroz@atgmail.com.

*(E.R.J.) E-mail: erin.johnson@dal.ca.

Notes

The authors declare no competing financial interest.

ACKNOWLEDGMENTS

We are grateful for financial support from the Natural Sciences and Engineering Research Council (NSERC), and for computational resources and support from ACEnet, Westgrid, and Compute Canada/Calcul Canada. We thank Sarah R. Whittleton for performing some preliminary calculations. L.M.L. would also like to acknowledge the Walter C. Sumner Foundation for financial support.

REFERENCES

- (1) Wheatley, P. J. The Crystal and Molecular Structure of Aspirin. *J. Chem. Soc.* **1964**, 6036–6048.
- (2) Ouyard, C.; Price, S. L. Toward Crystal Structure Prediction for Conformationally Flexible Molecules: The Headaches Illustrated by Aspirin. *Cryst. Growth Des.* **2004**, *4*, 1119–1127.
- (3) Vishweshwar, P.; McMahon, J. A.; Oliveira, M.; Peterson, M. L.; Zaworotko, M. J. The Predictably Elusive Form II of Aspirin. *J. Am. Chem. Soc.* **2005**, *127*, 16802–16803.
- (4) Bond, A. D.; Boese, R.; Desiraju, G. R. On the Polymorphism of Aspirin. *Angew. Chem., Int. Ed.* **2007**, *46*, 615–617.
- (5) Bond, A. D.; Boese, R.; Desiraju, G. R. On the Polymorphism of Aspirin: Crystalline Aspirin as Intergrowths of Two “Polymorphic” Domains. *Angew. Chem., Int. Ed.* **2007**, *46*, 618–622.
- (6) Bond, A. D.; Solanko, K. A.; Parsons, S.; Redder, S.; Boese, R. Single Crystals of Aspirin Form II: Crystallization and Stability. *CrystEngComm* **2011**, *13*, 399–401.
- (7) Varughese, S.; Kiran, M. S. R. N.; Solanko, K. A.; Bond, A. D.; Ramamurthy, U.; Desiraju, G. R. Interaction Anisotropy and Shear Instability of Aspirin Polymorphs Established by Nanoindentation. *Chem. Sci.* **2011**, *2*, 2236–2242.
- (8) Wen, S.; Beran, G. J. O. Accidental Degeneracy in Crystalline Aspirin: New Insights from High-Level *ab Initio* Calculations. *Cryst. Growth Des.* **2012**, *12*, 2169–2172.

- (9) Huang, Y.; Shao, Y.; Beran, G. J. O. Accelerating MP2C Dispersion Corrections for Dimers and Molecular Crystals. *J. Chem. Phys.* **2013**, *138*, 224112.
- (10) Chan, E. J.; Welberry, T. R.; Heerdegen, A. P.; Goossens, D. J. Diffuse Scattering Study of Aspirin Forms (I) and (II). *Acta Crystallogr., Sect. B: Struct. Sci.* **2010**, *66*, 696–707.
- (11) Crowell, E. L.; Dreger, Z. A.; Gupta, Y. M. High-Pressure Polymorphism of Acetylsalicylic Acid (Aspirin): Raman Spectroscopy. *J. Mol. Struct.* **2015**, *1082*, 29–37.
- (12) Das, D.; Desiraju, G. R. Packing Modes in Some Mono- and Disubstituted Phenylpropionic Acids: Repeated Occurrence of the Rare *syn,anti* Catemer. *Chem. - Asian J.* **2006**, *1*, 231–244.
- (13) Bürgi, H.-B.; Hostettler, M.; Birkedal, H.; Schwarzenbach, D. Stacking Disorder: The Hexagonal Polymorph of Tris(Bicyclo[2.1.1]hexeno)benzene and Related Examples. *Z. Kristallogr.* **2005**, *220*, 1066–1075.
- (14) Bauer, J. D.; Haussühl, E.; Winkler, B.; Arbeck, D.; Milman, V.; Robertson, S. Elastic Properties, Thermal Expansion, and Polymorphism of Acetylsalicylic Acid. *Cryst. Growth Des.* **2010**, *10*, 3132–3140.
- (15) Reilly, A. M.; Tkatchenko, A. Role of Dispersion Interactions in the Polymorphism and Entropic Stabilization of the Aspirin Crystal. *Phys. Rev. Lett.* **2014**, *113*, 055701.
- (16) Day, G. M.; Price, S. L.; Leslie, M. Elastic Constant Calculations for Molecular Organic Crystals. *Cryst. Growth Des.* **2001**, *1*, 13–27.
- (17) Wildfong, P. L. D.; Morris, K. R.; Anderson, C. A.; Short, S. M. Demonstration of a Shear-Based Solid-State Phase Transformation in a Small Molecular Organic System: Chlorpropamide. *J. Pharm. Sci.* **2007**, *96*, 1100–1113.
- (18) Roberts, R. J.; Rowe, R. C.; York, P. The Relationship Between Indentation Hardness of Organic Solids and Their Molecular Structure. *J. Mater. Sci.* **1994**, *29*, 2289–2296.
- (19) Bond, A. D.; Boese, R.; Desiraju, G. R. What is a Polymorph? Aspirin as a Case Study. *Am. Pharm. Rev.* **2007**, *10*, 24–30.
- (20) Allen, F. H. The Cambridge Structural Database: a Quarter of a Million Crystal Structures and Rising. *Acta Crystallogr., Sect. B: Struct. Sci.* **2002**, *58*, 380–388.
- (21) Aspirin form-I: CCDC number 610952/CSD refcode ACSALA14. Aspirin form-II: CCDC number 617840/CSD refcode ACSALA22. Crystal structures can be obtained free of charge from The Cambridge Crystallographic Data Centre via www.ccdc.cam.ac.uk/data_request/cif.
- (22) Giannozzi, P.; Baroni, S.; Bonini, N.; Calandra, M.; Car, R.; Cavazzoni, C.; Ceresoli, D.; Chiarotti, G. L.; Cococcioni, M.; Dabo, I.; Dal Corso, A.; Fabris, S.; Fratesi, G.; de Gironcoli, S.; Gebauer, R.; Gerstmann, U.; Gougousis, C.; Kokalj, A.; Lazzeri, M.; Martin-Samos, L.; Marzari, N.; Mauri, F.; Mazzarello, R.; Paolini, S.; Pasquarello, A.; Paulatto, L.; Sbraccia, C.; Scandolo, S.; Sclauzero, G.; Seitsonen, A. P.; Smogunov, A.; Umari, P.; Wentzcovitch, R. M. QUANTUM ESPRESSO: a Modular and Open-Source Software Project for Quantum Simulations of Materials. *J. Phys.: Condens. Matter* **2009**, *21*, 395502.
- (23) Blöchl, P. E. Projector Augmented-Wave Method. *Phys. Rev. B: Condens. Matter Mater. Phys.* **1994**, *50*, 17953–17979.
- (24) Becke, A. D. On the Large-Gradient Behavior of the Density Functional Exchange Energy. *J. Chem. Phys.* **1986**, *85*, 7184–7187.
- (25) Perdew, J. P.; Burke, K.; Ernzerhof, M. Generalized Gradient Approximation Made Simple. *Phys. Rev. Lett.* **1996**, *77*, 3865–3868.
- (26) Becke, A. D.; Johnson, E. R. Exchange-Hole Dipole Moment and the Dispersion Interaction Revisited. *J. Chem. Phys.* **2007**, *127*, 154108.
- (27) Otero-de-la-Roza, A.; Johnson, E. R. Van der Waals Interactions in Solids Using the Exchange-Hole Dipole Moment Model. *J. Chem. Phys.* **2012**, *136*, 174109.
- (28) Otero-de-la-Roza, A.; Johnson, E. R. A Benchmark for Non-Covalent Interactions in Solids. *J. Chem. Phys.* **2012**, *137*, 054103.
- (29) Togo, A.; Tanaka, I. First Principles Phonon Calculations in Materials Science. *Scr. Mater.* **2015**, *108*, 1–5.
- (30) Hill, R. The Elastic Behaviour of a Crystalline Aggregate. *Proc. Phys. Soc., London, Sect. A* **1952**, *65*, 349–354.
- (31) de Jong, M.; Chen, W.; Angsten, T.; Jain, A.; Notestine, R.; Gamst, A.; Sluiter, M.; Ande, C. K.; van der Zwaag, S.; Plata, J. J.; Toher, C.; Curtarolo, S.; Ceder, G.; Persson, K. A.; Asta, M. Charting the Complete Elastic Properties of Inorganic Crystalline Compounds. *Sci. Data* **2015**, *2*, 150009.
- (32) Perlovich, G. L.; Kurkov, S. V.; Kinchin, A. N.; Bauer-Brandl, A. Solvation and Hydration Characteristics of Ibuprofen and Acetylsalicylic Acid. *AAPS PharmSci* **2004**, *6*, 22–30.
- (33) Li, T.; Feng, S. Empirically Augmented Density Functional Theory for Predicting Lattice Energies of Aspirin, Acetaminophen Polymorphs, and Ibuprofen Homochiral and Racemic Crystals. *Pharm. Res.* **2006**, *23*, 2326–2332.
- (34) Otero-de-la-Roza, A.; Cao, B. H.; Price, I. K.; Hein, J. E.; Johnson, E. R. Density-Functional Theory Predicts the Relative Solubilities of Racemic and Enantiopure Crystals. *Angew. Chem., Int. Ed.* **2014**, *53*, 7879–7882.
- (35) Beyer, T.; Price, S. L. The Errors in Lattice Energy Minimisation Studies: Sensitivity to Experimental Variations in the Molecular Structure of Paracetamol. *CrystEngComm* **2000**, *2*, 183–190.
- (36) Li, T. Understanding the Polymorphism of Aspirin with Electronic Calculations. *J. Pharm. Sci.* **2007**, *96*, 755–760.
- (37) Charlier, J.-C.; Gonze, X.; Michenaud, J.-P. First-Principles Study of the Stacking Effect on the Electronic Properties of Graphite(s). *Carbon* **1994**, *32*, 289–299.
- (38) Lipson, H.; Stokes, A. R. The Structure of Graphite. *Proc. R. Soc. London, Ser. A* **1942**, *181*, 101–105.
- (39) Desiraju, G. R. Crystal Engineering: From Molecules to Crystal. *J. Am. Chem. Soc.* **2013**, *135*, 9952–9967.
- (40) Otero-de-la-Roza, A.; Johnson, E. R. Non-Covalent Interactions and Thermochemistry using XDM-Corrected Hybrid and Range-Separated Hybrid Density Functionals. *J. Chem. Phys.* **2013**, *138*, 204109.
- (41) Henkelman, G.; Uberuaga, B. P.; Jónsson, H. A Climbing Image Nudged Elastic Band Method for Finding Saddle Points and Minimum Energy Paths. *J. Chem. Phys.* **2000**, *113*, 9901–9904.
- (42) Henkelman, G.; Jónsson, H. Improved Tangent Estimate in the Nudged Elastic Band Method for Finding Minimum Energy Paths and Saddle Points. *J. Chem. Phys.* **2000**, *113*, 9978–9985.
- (43) Qian, G.-R.; Dong, X.; Zhou, X.-F.; Tian, Y.; Oganov, A. R.; Wang, H.-T. Variable Cell Nudged Elastic Band Method for Studying Solid-Solid Structural Phase Transitions. *Comput. Phys. Commun.* **2013**, *184*, 2111–2118.
- (44) Krausz, A. S.; Eyring, H. Chemical Kinetics of Plastic Deformation. *J. Appl. Phys.* **1971**, *42*, 2382–2385.
- (45) Kim, Y.; Machida, K.; Taga, T.; Osaki, K. Structure Redetermination and Packing Analysis of Aspirin Crystal. *Chem. Pharm. Bull.* **1985**, *33*, 2641–2647.
- (46) Riedo, E.; Gnecco, E.; Bennewitz, R.; Meyer, E.; Brune, H. Interaction Potential and Hopping Dynamics Governing Sliding Friction. *Phys. Rev. Lett.* **2003**, *91*, 084502.
- (47) Szlufarska, I.; Chandross, M.; Carpick, R. W. Recent Advances in Single-Asperity Nanotribology. *J. Phys. D: Appl. Phys.* **2008**, *41*, 123001.